

# New technological developments in Integral Field Spectroscopy

S. Vives\*<sup>a</sup>, E. Prieto<sup>a</sup>, Y. Salaun\*\*<sup>b</sup>, P. Godefroy<sup>b</sup>

<sup>a</sup> Laboratoire d'Astrophysique de Marseille (LAM), Technopole Marseille-Etoile, France;

<sup>b</sup> Winlight Optics, ZA St Martin, 84120 Pertuis, France

## ABSTRACT

Integral Field Spectroscopy (IFS) provides a spectrum simultaneously for each spatial sample of an extended two-dimensional field. Basically, the IFS is located in a telescope focal plane and is composed by an Integral Field Unit (IFU or image slicer) and a spectrograph. The IFU acts as a coupler between the telescope and the spectrograph by reformatting optically a rectangular field into a quasi-continuous pseudo-slit located at the entrance focal plane of the spectrograph. The Integral Field Units (IFUs) are presently limited either by their cost/risk (when manufactured with classical glass polishing techniques) or by their performances (when constituted by metallic components).

Recent innovative methods, developed conjointly by LAM (Laboratoire d'Astrophysique de Marseille, France) and WinLight Optics (Marseille, France), allow reaching high performances (accurate roughness, sharp edges, surface form, etc.) with standard glass manufactured components while saving costs and time by an order of magnitude compared with classical techniques. Last developments (in term of design and manufacturing) and applications are presented in details in this article.

**Keywords:** Integral Field Unit, IFU, Integral Field Spectroscopy, IFS, image slicer, classical polishing

## 1. INTRODUCTION

An Integral Field Spectrograph (IFS) reconstructs the data cube containing the two spatial directions X and Y plus the wavelength direction, providing simultaneously the spectrum for each spatial pixel in the 2D field. All IFS are made of two successive stages: (i) the spatial stage that reformats the field of view (also called, Integral Field Unit or IFU); and (ii) the classical spectral stage that disperses and focuses the light on the detector. The spatial stage is the most critical part of the IFS.

There are several types of IFU based either on lenslet array, fiber array or image slicer. The latter is the most promising solution since it optimizes spatial and spectral information (most efficient use of detector pixels) in the data cube while operating in space and cryogenic environments. The image slicer also minimizes optical losses and improves the efficiency and compactness of the system.

As shown Fig.1, an image slicer has two main functions: (i) transform the rectangular field of view into a series of sub-slits that forms the entrance classical slit of the spectrograph (spectral stage); and (ii) re-image the input pupil of the telescope at the entrance pupil of the spectrograph. The main component of an image slicer is the slicer mirror. It consists of a stack of several thin mirrors (called slices), powered or not with a particular orientation in order to redirect the light in different directions.

Although planned to be implemented on several future ground-based and space instruments (e.g. SNAP<sup>[1]</sup>, MUSE<sup>[2]</sup>, EAGLE<sup>[3,4]</sup>), manufacturing at an affordable cost and time such a component remains a major challenge.

We propose an alternative method (from design to manufacturing) which achieves highest optical performances ever-realized on slicer mirrors while making costs very competitive.

In this article, we present a new approach using glass standard polishing which reconciles high opto-mechanical performances and low risk/cost manufacturing processes.

\* Sebastien.Vives@oamp.fr; phone: +33-(0)4-91-05-69-31; \*\* yves.salaun@winlight-optics.com; phone: +33-(0)4-90-07-78-63

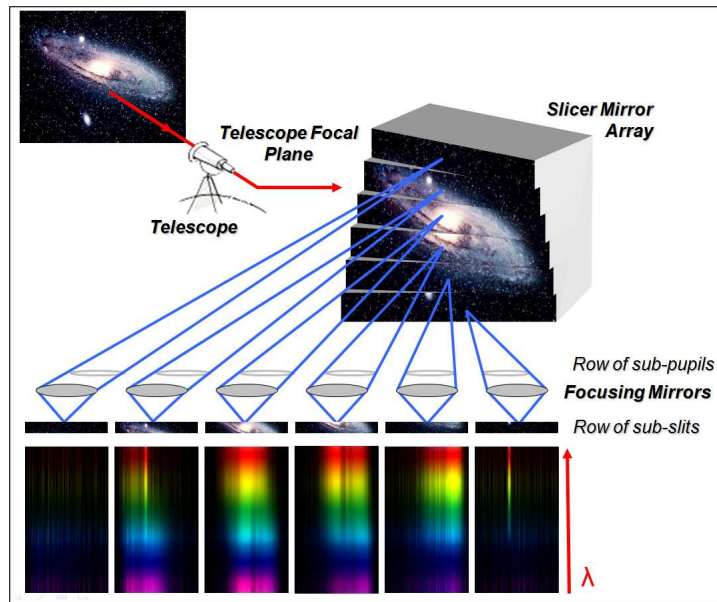


Fig. 1. Image slicer concept. The field of view is divided into N strips on a slicer mirror (here N=6). Each of N slices re-images the telescope pupil, so there are N images in the pupil plane. Because of a tilt adapted to each individual slice, the N images are arranged by the Focusing Mirrors along a line and form a long pseudo-slit (i.e. row of sub-slits).

## 2. AN INNOVATIVE METHOD: DESCRIPTION

Classically slices are individually polished while our alternative method intends to manufacture one or more stacks of slices by a single polishing process. Fig.2 schematically describes main steps of manufacturing process:

- a) Plane rectangular slices are massively produced by classical polishing and cutting processes with respect to tight thickness, parallelism, and perpendicularity requirements. Back and lateral sides serve as reference surfaces during next processes.
- b) All slices are arranged and maintained by optical contact. Because of the use of optical contact, the block constituted by slices is equivalent to the blank of glass used in the traditional polishing of more classical mirrors. The position of the vertexes of each slice on the block is known with a very high accuracy with respect to the borders of the block and it will depend on the final orientation of each active surface in the slicer mirror.
- c) The block constituted by slices is polished thanks to standard polishing techniques to achieve the required shape (either spherical or aspherical, see section 6.2). After that, the block is dismantled in order to obtain all individual polished slices (after only one polishing process).
- d) Slices are re-arranged by block or individually (depending on the design) to get one or more final stacks of slices.

All these steps are overcome by Winlight Optics. Individual slices or blocks are stacked in a "blind" process during which metrology is not required allowing fast stacking process. The current stacking process only takes few hours for a dozen of slices with some simple manipulations.

All slices are maintained by optical contact. The choice of optical contact between slices allows insuring both the cohesion into the optical assembly and the preservation of the alignment. Furthermore, the internal stress of each slice remains constant from the polishing to the stacking (final positioning in the instrument). This point is crucial to preserve the optical quality of the system.

All slices have the same curvature and their orientations are strongly dependent on their positions on the block. Furthermore, vertexes of each slice are located on the same sphere (or asphere). Because these characteristics impose severe constraints on the optical design, we also developed numerical tools<sup>[5]</sup> to design IFUs using our manufacturing technique. These tools are based on the User Defined Surface USD-DLL capability of Zemax and allow to automatically stacking up all slices in function of their arrangement on the block used to polish them. Basically, the user specifies or optimizes on manufacturing's parameters (such as positions of particular slices on the block) and the USD-DLL computes the corresponding slicer mirror. These tools make straightforward the implementation of a slicer mirror based on our method.

The optical quality of each slice is ultimate, thanks to the simplicity of the process and the very well known techniques employs to manufacture them (standard machining and polishing).

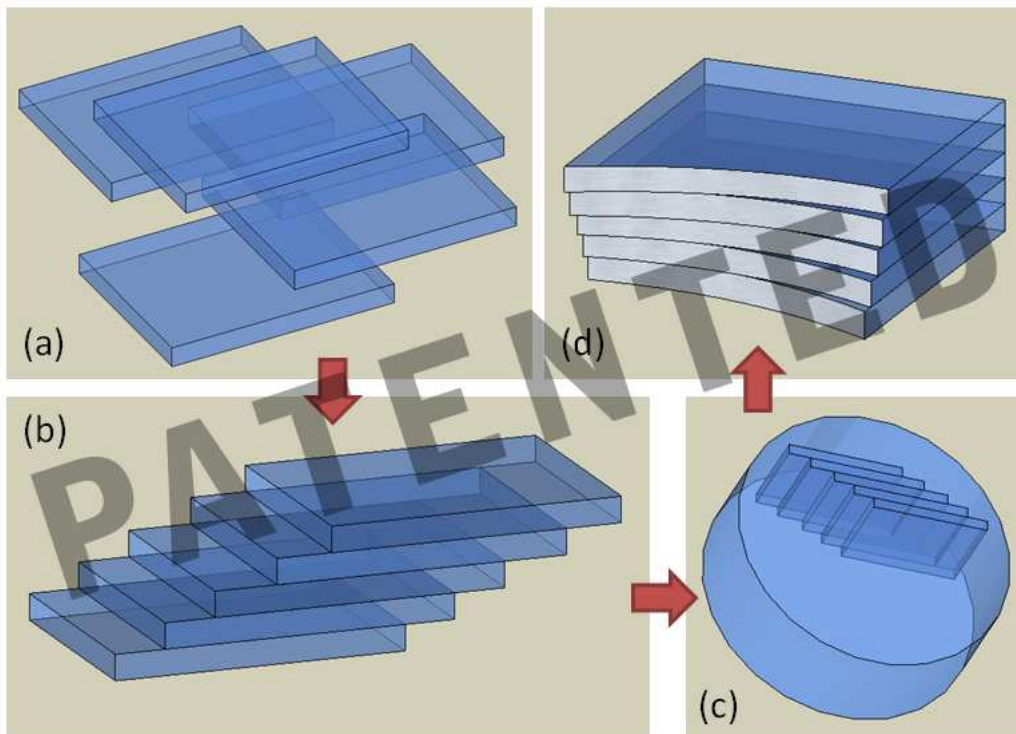


Fig. 2. Schematic view of the main steps of the manufacturing process. All slices (a) are distributed on the block (b) used to polish them (c) and are re-arranged after to build the final stack of slices (d).

### 3. AN INNOVATIVE METHOD: MEASURED PERFORMANCES

In 2006, in order to validate our numerical tools and manufacturing method, we realized a demonstrator constituted by 6 actives slices (Fig. 3). Table 1 summarizes optical performances measured on this demonstrator. Our method provides well known results in terms of surface shape quality (section 3.1) and surface roughness (section 3.2). We also discuss the quality achieved on edges (section 3.3) and the angular errors of the slices (section 3.4). Note that in terms of performances there are no further limitations except the inherent limitations of standard polishing.

Table. 1. Summary of optical performances typically reached with our method. This innovative method provides well known performances since it is based on classical polishing techniques. It is interesting to note that because all slices are produced during the same process all the above performances are homogeneous over all slices.

Surface shape accuracy	$\lambda/100$ rms
Surface roughness	$<0.4$ nm
Edges quality	from $1 \mu\text{m}$ to $5 \mu\text{m}$
Tilt error of slices	$< 15$ arcsec PTV

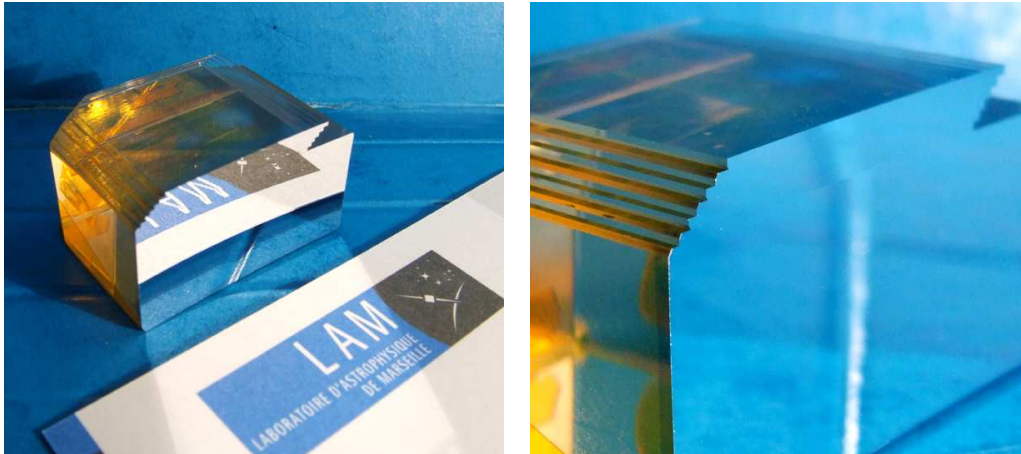


Fig. 3. Slicer mirror demonstrator designed by LAM and manufactured by Winlight Optics. It is composed of 6 slices ( $0.5 \times 23 \text{mm}$ ). Note that slices are stacked to show the disposition of slices on the block during polishing.

### 3.1 Surface shape accuracy

The surface shape directly affects the image quality and the Point Spread Function (PSF) shape. We demonstrated that ultimate results obtained with the standard glass polishing process on classical mirrors, are equally obtained on slices. The typical surface quality accuracy achieved by standard polishing is  $\lambda/100$  RMS and  $\lambda/20$  PTV ( $\lambda=632.8$  nm).

The FWHM PSF measurements made on standard glass polished slicer mirror differ from the theoretical PSF by less than 5%. The image quality is good enough whatever the PSF is sliced or not. Note that measurements made at cryogenic temperature (50 K) have also shown the stability of the PSF compared to the PSF at room temperature <sup>[6]</sup>.

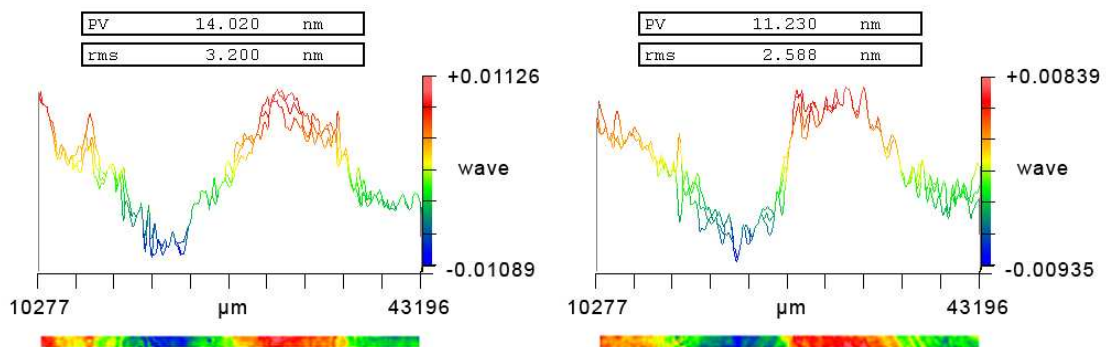


Fig. 4. Examples of measurements of surface shape of two slices of the MUSE demonstrator (see section 5). Surface form accuracies are better than  $\lambda/100$  RMS and  $\lambda/20$  PTV. Note that there is scale factor of 0.5 in the two graphics.

### 3.2 Surface roughness

The surface roughness of optical surfaces introduces scattered light in the optical path and reduces overall throughput of the instrument.

Commonly, a roughness of 0.3-0.4 nm is reached on spherical or aspherical surfaces. Because slices are polished in the same classical way than other more classical optics, the roughness of the active surface of slices is typically in the same range. The tools used during the polishing process are larger compared to the dimension of one thus avoiding grooves or marks on the active surface. The variation in the surface roughness from one slice to the other are minimized since they are polished together. This ensures better throughput uniformity in the field of view of the instrument.

Fig. 5 shows an example of roughness measurements made on the demonstrator realized in 2006.

Note that although lower surface roughness can be achieved, it is already one order one magnitude below those obtained by all other manufacturing processes (diamond turning, raster fly-cutting or replication).

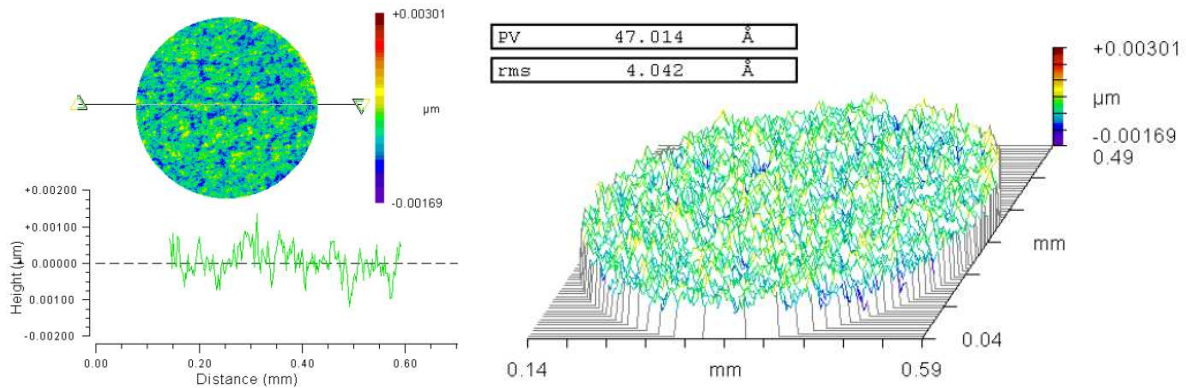


Fig. 5. Example of surface roughness measurement made on a small portion (450x450 $\mu\text{m}$ ) of one slice.

### 3.3 Edges quality

Edges are transition regions located within the field of view. They mainly present a source of both reduction in throughput and increase in scattered light.

We concentrated our efforts on edges preservation during all manufacturing steps and now we commonly achieve edge thickness less than 5 $\mu\text{m}$  with a very low number of marks.

### 3.4 Component geometry errors

Component geometry corresponds to the positioning and alignment of each slice with respect to an opto-mechanical reference located on one side (back or lateral) of the slicer mirror.

The errors on the component geometry define the envelope where are located center of curvature of each slice with respect to the opto-mechanical reference. They include both: (i) errors on slice manufacturing (dimensions, thickness, parallelism, and perpendicularity); and (ii) errors on slice positioning in the stack.

It is also important to note that optical contact also preserve alignment at cryogenic temperatures.

In order to illustrate the expertise of Winlight Optics in this domain, we can cite the “échelle” component (Fig. 6) developed for the French spatial agency (CNES). It is composed of 24 thin flat mirrors (4 mm thick and 90mm width). The parallelism between two consecutive mirrors is less than  $\pm 2$  arcsec PTV ( $\pm 1.2$  arcsec RMS). The absolute position of each surface (height of each step) has been controlled to  $\pm 1.5 \mu\text{m}$  PTV. The difference of the thickness between such a component and a slicer mirror (about few millimeters against half a millimeter) doesn't impact the performances achieved.

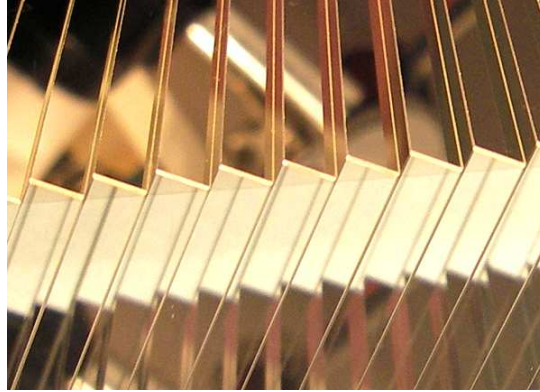


Fig. 6. View of one echelette mirrors developed by Winlight Optics for CNES. Only few mirrors are visible.

#### 4. SPACE-QUALIFIED SLICER MIRRORS

In the context of the SNAP (SuperNova Acceleration Probe) mission, LAM has developed a breadboard dedicated to the space-qualification of the glass-based slicer mirror. The qualification of the optical component (i.e. the slicer mirror itself) is strongly dependant to its opto-mechanical mount.

LAM proposed to support the Zérodur assembly thanks to a monolithic invar mount equipped with three bipods (see Fig.7). The slicer mirror consists of both 60 slices (0.5x20x20mm, only 10 actives) and two additional pieces of Zérodur allowing safe interfacing between the optical and mechanical parts. These two pieces have been designed to reduce stress propagation from bipods to the slices assembly.

We demonstrated that glass-based slicer mirrors are compatible with space constraints (mechanical and thermal environments). Please refer to <sup>[7]</sup> if you wish further information.

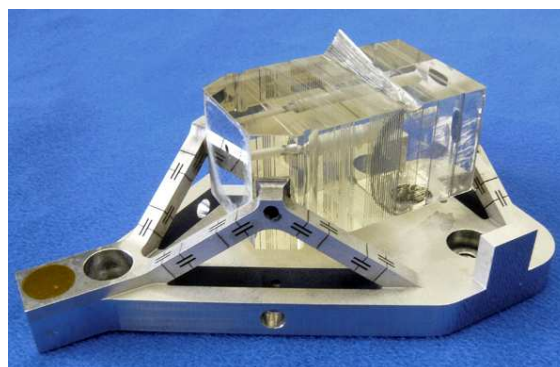


Fig. 7. Monolithic invar mount supporting the 60 slices assembly. Mechanical and thermal tests realized at LAM have demonstrated the aptitude of the glass-based slicer mirror to be implemented on space instrumentation.

## 5. CURRENT APPLICATION: THE MUSE DEMONSTRATOR

Proposed for the second generation VLT-instrumentation, MUSE (Multi-Unit Spectroscopic Explorer) is an Integral Field Spectrometer (IFS) proposed by CRAL (Centre de Recherche Astronomique de Lyon) for a first light in 2012<sup>[2]</sup>.

It is composed of 24 identical IFUs. The field of view to be sliced, by each IFU, is unusually large leading to a specific configuration of the stack of slices.

The slicer mirror is composed of 4 classical slicer mirrors stacks side by side. Each of them is constituted by 12 slices polished all together at the same time. They have a radius of curvature of 300mm and are distributed on the block during polishing as shown Fig.8. They are 33.4mm long and 0.925 mm thick.

Performances achieved with this demonstrator are within the specifications and are listed in Table 2.

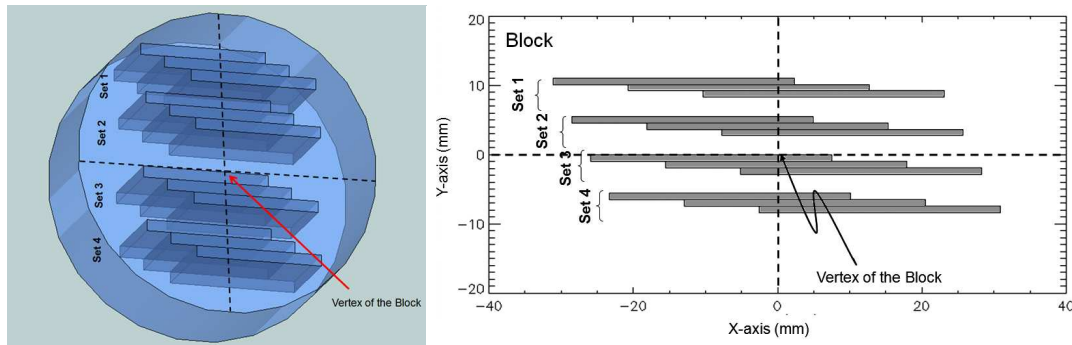


Fig. 8. Arrangement of the slices on the block during polishing. The 12 slices are distributed in 4 sub-assemblies of 3 slices each. The 4 slicer mirrors are identical and has the same arrangement.

Table 2. Overall MUSE IFU (slicer mirror plus Focusing Mirrors) performances. The X-axis is along the spatial direction while the Y-axis is along the spectral direction.

<b>Relative location of pseudo-slit</b>	Max error along X-axis	30 $\mu\text{m}$
	RMS error along X-axis	10 $\mu\text{m}$
	Max error along Y-axis	120 $\mu\text{m}$
	RMS error along Y-axis	20 $\mu\text{m}$
<b>Point Spread Function</b>	89 $\pm$ 3% of energy is focused in pseudo-slits (35 $\mu\text{m}$ x 70 $\mu\text{m}$ )	

On top of slices manufacturing, we also designed and manufactured focusing mirrors for the MUSE prototype (Fig. 12). As shown Fig.1, focusing mirrors are used to re-image sub-pupils and sub-slits after the slicer mirror. In that concept, all focusing mirrors are strictly identical (same curvature, same orientation) allowing mass production of such a mirrors. To control mirrors orientation, each spherical mirror is decentered in order to displace its vertex with respect to the corresponding incident chief ray. This lead to oversized mirrors accurately all together maintained by a precise opto-mechanical mounting.

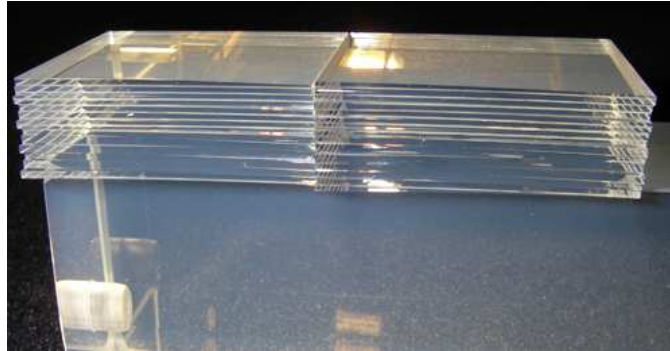


Fig.9. Partial arrangement of the MUSE slicer mirror. Only two stacks (2 x 12 slices) are implemented on the support. Note that slices are stacked without coating.

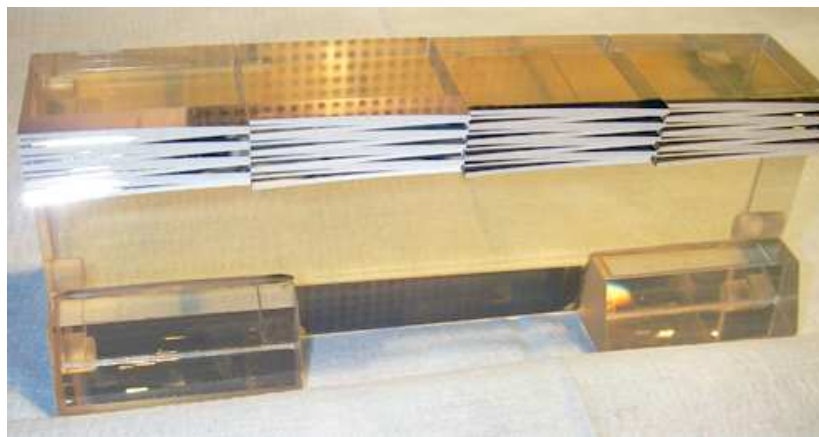


Fig.10. Final arrangement of the MUSE slicer mirror. It is composed of four slicer mirrors stacked side-by-side. It is overall length is about 130 mm.

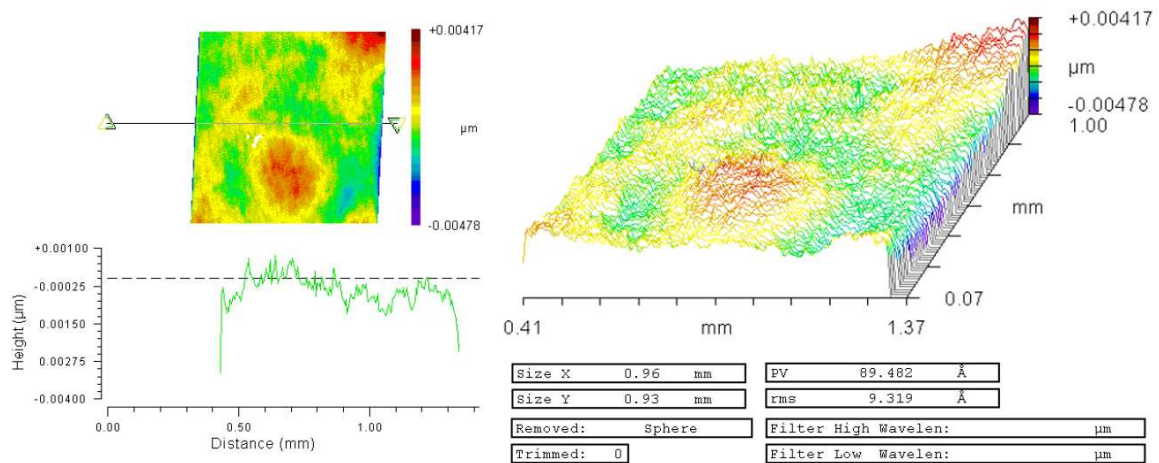


Fig. 11. Measurement of the surface shape accuracy of one slice of the MUSE slicer mirror. Note that the measure is made without filter (only the sphere is removed) on a large area (960x930µm) equivalent to one pixel of MUSE.



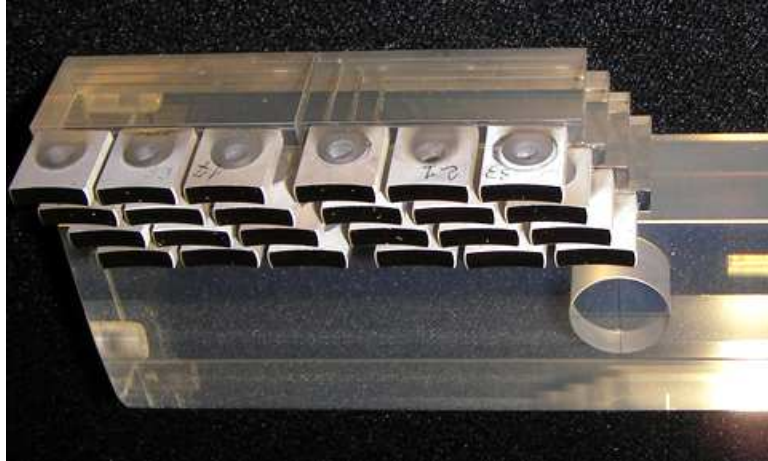


Fig.12. Focusing Mirror Array (FMA) for the MUSE IFU. Only the 24 first mirrors are arranged. All mirrors are strictly identical and their orientation is controlled by their position with respect to the incident chief rays.

## 6. FUTURE DEVELOPMENTS

### 6.1 New materials

Up to now, all slices were made of Zérodur because it ensures both the preservation of the optical properties of the slicer mirror at all temperatures (low coefficient of thermal expansion) and the manufacturability of the slicer mirror.

However, we began to explore the possibility to manufacture slicer mirror made of ceramic material such as SiC. This will facilitate the opto-mechanical implementation of the slicer mirror in cryogenic environment since the support of the slicer mirror can also be made of SiC.

The first prototype was realized in 2007 and the first results have been successful in term of sharp edge quality. Since, this program has been delayed because of the MUSE demonstrator.

### 6.2 Aspherical shapes

Up to now all slicer mirrors are based on plane or spherical shapes whatever the manufacturing technique (glass polishing or diamond machining).

Glass-based slicer mirrors are only limited by management aspects (time, cost, risk) and not by technical aspects (feasibility). Indeed, when all slices are individually polished it is a long and burden task to manufacture one slicer mirror. Non-spherical shape imposes additional constraints which strongly increase manufacturing time.

Because our alternative method limits the number of polishing, it is possible to envisage polishing aspherical shapes without additional risks. On top of traditional polishing processes, other techniques (such as ion-beam polishing, robot) can be employed to manufacture future glass-based high quality slicer mirrors. We will explore this innovative aspect in the coming months.

## 7. CONCLUSION

In the past, slicer mirrors based on glass polishing have demonstrated their superiority in terms of performances compared with all other manufacturing techniques (diamond turning, raster fly-cutting or replication). Now by proposing an alternative method of designing and manufacturing such a slicer mirror, glass-based slicer mirrors outperform all its competitors in terms of both optical performances and costs.

## REFERENCES

- [1] Prieto E. et al., “An image slicer spectrograph for the SNAP/JDEM mission”, paper 7010-44, this conference (2008).
- [2] Bacon R., “The MUSE second-generation VLT instrument”, paper 7014-15, this conference (2008).
- [3] Cuby J.G., et al., “EAGLE: the wide-field multi-IFU NIR spectrograph for the European ELT”, paper 7014-54, this conference (2008).
- [4] Prieto E., et al., “Optical solutions for the multi-IFU instrument EAGLE for the European ELT”, paper 7014-55, this conference (2008)
- [5] Vives S., et al., “A set of Zemax user-defined surfaces to model slicer mirrors”, Proc. SPIE, 6273 (2006)
- [6] Laurent F. et al., “Designing, manufacturing, and testing of an advanced image slicer prototype for the James Webb Space Telescope”, Proc. SPIE, 5494 (2004)
- [7] Pamplona T. et al., “Three bipods design support for an image slicer”, paper 7018-82, this conference (2008)